

2004

Optimization of Scroll Compressor Involute Height with Machining Considerations

Brian VanderKooy
Trane Company

Follow this and additional works at: <https://docs.lib.purdue.edu/icec>

VanderKooy, Brian, "Optimization of Scroll Compressor Involute Height with Machining Considerations" (2004). *International Compressor Engineering Conference*. Paper 1634.
<https://docs.lib.purdue.edu/icec/1634>

This document has been made available through Purdue e-Pubs, a service of the Purdue University Libraries. Please contact epubs@purdue.edu for additional information.

Complete proceedings may be acquired in print and on CD-ROM directly from the Ray W. Herrick Laboratories at <https://engineering.purdue.edu/Herrick/Events/orderlit.html>

OPTIMIZATION OF SCROLL COMPRESSOR INVOLUTE HEIGHT WITH MACHINING CONSIDERATIONS

Brian VANDERKOOY

Trane, Engineering Technology
LaCrosse, WI, USA
p: 608-787-2670, f: 608-787-2669, bvanderkooy@trane.com

ABSTRACT

The optimization of scroll compressor performance requires selection of an involute height to minimize parasitic losses, while not creating undue machining difficulty. Selection of short involutes results in increased thrust bearing losses. The use of tall involutes leads to increased leakage area through the minimum flank gap and higher gas loads at the radial bearings. Selection of tall involutes also increases the potential for scrap generation by requiring the use of a mill which is longer, and possibly smaller in diameter.

This paper discusses a method for the selection of an optimum involute height based on consideration of parasitic losses and machining capability. The values of involute stress, journal bearing film thickness, discharge port area, suction volume, and volume ratio are held constant in this study.

1. INTRODUCTION

Many published works exist presenting methods for selecting an optimum scroll involute design. Included are methods which fix capacity, wrap thickness, and volume ratio (Etemad and Nieter, 1988); methods which fix the number of wraps and wrap thickness (Ishii *et al.*, 1992); and methods which fix cylinder diameter, (package size in the radial direction), and wrap thickness (Ishii *et al.*, 1994). The approach described in this paper is different in that several engineering parameters are held constant. The non-linear Engineering Equation Solver (EES) was used to solve simultaneous equations to generate candidate geometries. These candidate geometries are then evaluated in a 1D model which evaluates the performance of each candidate design at the ARI rating point of 45°F (7.2°C) saturated suction temperature, 130°F (54.4°C) saturated discharge temperature, and 20°F (11.1°C) return gas superheat. This paper will not discuss the details of the performance model. It will instead focus on the method used to generate candidate geometries and the performance characteristics of the results.

In addition to the performance analysis results, a model of mill deflection will be presented. The mill deflection model will provide an estimate of mill deflection for candidate geometries. The optimum involute geometry is one which achieves near maximum performance while minimizing machining difficulty and scrap generation.

2. ANALYSIS METHOD

In order to develop the candidate geometries, several design constraints were made. These following parameters were kept constant:

- Suction volume. A constant suction volume constraint creates candidate geometries of the same nominal capacity.
- Volume ratio. The volume ratio is selected based on the refrigerant and the design operating conditions.
- Involute stress level. Previously published papers typically present an optimization method which assumes constant involute thickness. Using a semi-empirical correlation developed through finite element analysis, a constant stress relationship for involute stress has been developed using involute height and gas load as inputs.
- Journal bearing film thickness. In order to accurately gauge the performance of each design, the bearing sizes are adjusted based on loading condition to maintain constant film thickness. A curve

fit of the charts developed by Raimondi and Boyd (1958) was used to provide an initial estimate of the required bearing size.

- Port area. The port area is also kept constant in this study. The port area selection is strongly correlated to the design operating condition and a representative value of port area was used in this analysis.
- Baseplate deflection. The baseplate deflection is calculated using Roark's formulas presented in Young's text (1989, p. 429). Superposition was used to account for the non-uniform loading.

Given these input constraints and equations which define the scroll geometric parameters, an equation set can be constructed which has only one involute geometry as a solution for a given value of involute height. This equation set involves equations which control the involute geometry, stress level, journal bearing film thickness, and baseplate deflection. The equations which model stress level, journal bearing film thickness, and baseplate deflection are basic models which allow the use of simplified equations. After a design is selected, more sophisticated analysis should be performed on the individual components to achieve a more refined design.

Twenty-five candidate geometries evenly distributed over a range of heights were created for analysis. The variation in geometric parameters of these candidate geometries is investigated in the next section of this paper. The variation of several geometric parameters has a significant impact on the performance model results. The performance results are discussed in section 4 with the optimum candidate from a performance standpoint being selected. The machinability of the candidate geometries will be considered in section 5. The maximum mill size and mill deflection for each candidate geometry will be estimated. Both performance and machining considerations will be applied to select the optimum geometry.

3. GEOMETRY RESULTS

The applied constraints on the design have an interesting impact on several scroll geometry parameters. The constant stress constraint becomes significant in determining the part mass as tall involutes are penalized through the addition of extra material to satisfy the constant stress requirement. The additional involute thickness increases the part weight. Since the involutes are becoming thicker, the orbiting scroll diameter does not decrease significantly. The initial constraint of constant port area also limits the change in generating radius. The changes in orbiting scroll diameter, generating radius, and involute thickness are shown in Figure 1.

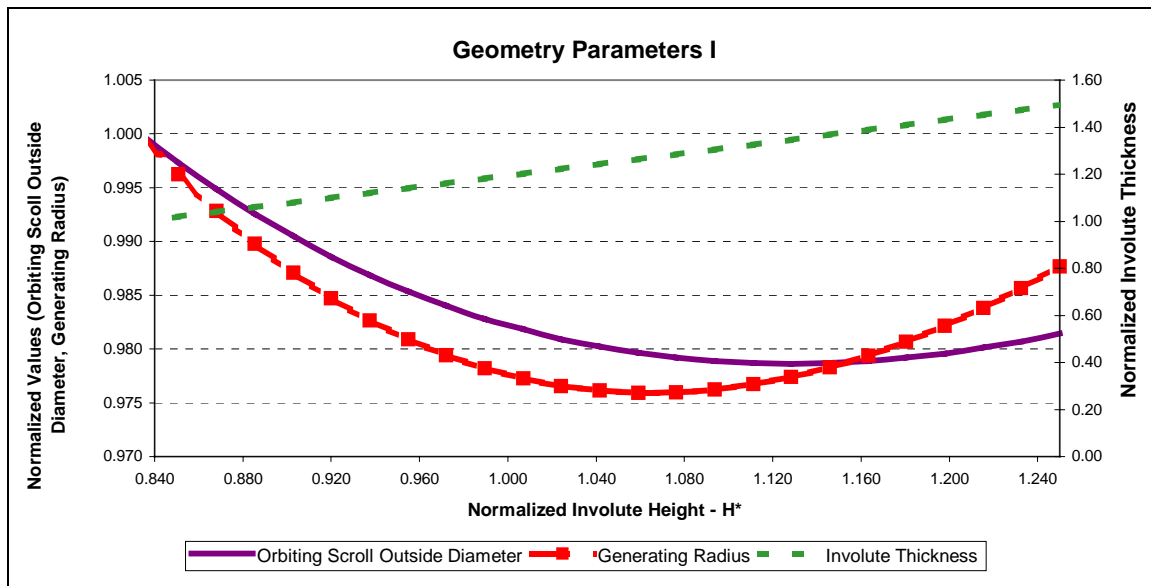


Figure 1. Change in orbiting scroll diameter, generating radius, and involute thickness.

While the mass of the orbiting scroll is increasing as the involutes become taller, largely due to the increase in involute thickness, the orbit radius is decreasing since the generating radius change is small as the involutes become thicker, as shown in Figure 1. The increasing mass of the orbiting scroll and the decreasing orbit

radius have opposite effects on the inertial load generated by the orbiting scroll. The result is a decrease in inertial load since the orbit radius is decreasing at a faster rate than the part mass is increasing. The changes in orbiting scroll mass, orbit radius, and orbiting scroll inertia are shown in Figure 2.

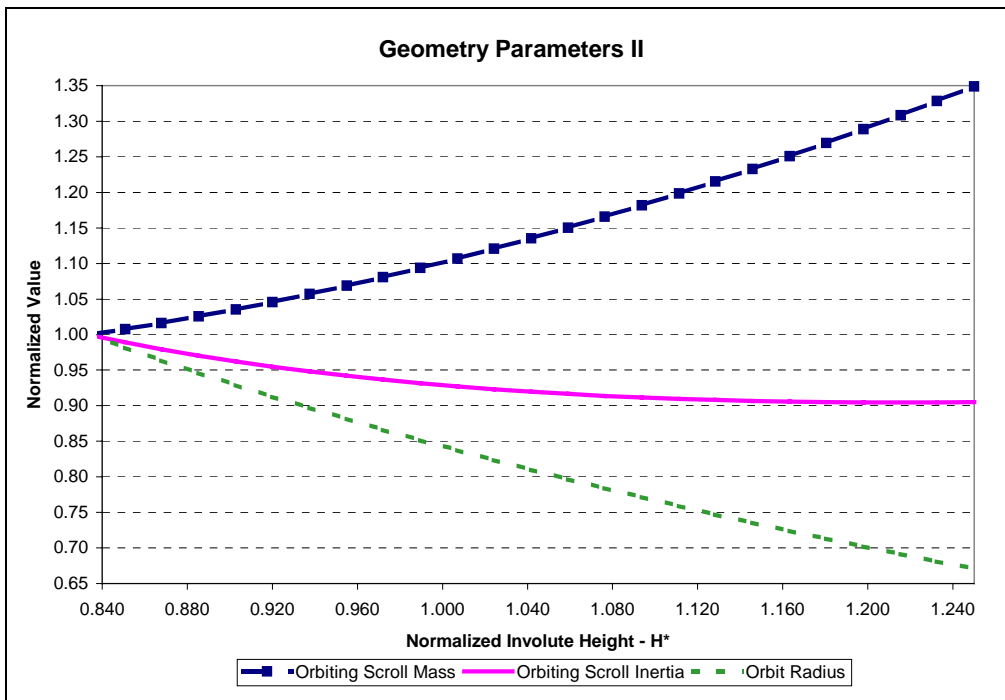


Figure 2. Change in orbiting scroll mass, orbiting scroll inertia, orbit radius.

Understanding the change in inertial load and orbit radius is important in understanding the bearing load and power consumption characteristics, which will be discussed in the next section.

4. PERFORMANCE RESULTS

The performance of each of the twenty-five candidate geometries was calculated at the ARI rating point using the 1D performance model. Evaluated in the performance model was the compression process including leakage, radial and thrust bearing losses, motor losses, pressure drops, friction, and heat transfer. The predicted effect of involute height on performance at the ARI rating point is shown in Figure 3.

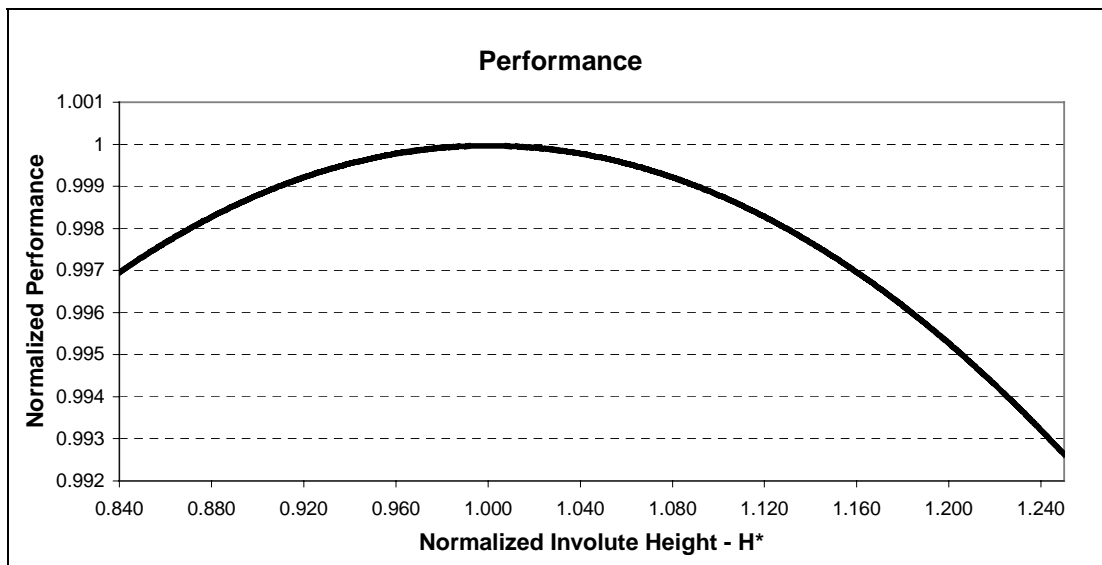


Figure 3. Performance results.

It is also important to note Figure 3 reveals the compressor performance could be characterized as not highly dependent on height over the selected height range. Therefore, moderate changes in involute height can be made without a significant performance penalty. Based on the results from the 1D model, the changes in the thrust bearing losses, main bearing losses, and leakage losses have the greatest effect on compressor performance. The reasons for the change in thrust bearing loss, main bearing loss, and leakage loss can be understood by considering the change in compressor geometry as a function of involute height and its impact on each loss. The thrust bearing will be the first of these components to be considered.

4.1 Thrust Bearing Performance

The thrust bearing power consumption is a function of the thrust load, thrust area, and surface tangential velocity. The power consumption is computed using a parallel plate friction loss model presented by Hemingway (1965-66). The performance model analyzes the design without any balance pistons. Therefore, the thrust bearing load is equivalent to the axial gas force (AGF) on the orbiting scroll. As the involutes become taller, it would be expected that the axial gas force would decrease. However, since the involute stress is kept constant, the AGF does not decrease significantly. This is because the overall scroll diameter is nearly constant, as shown in the previous section of this paper. The minimal change in diameter also results in a nearly constant thrust area. However, as presented in the previous section, the orbit radius, and therefore the tangential velocity, is decreasing significantly. As a result, the decrease in orbit radius results in a decrease in thrust bearing power consumption. The change in thrust bearing power is illustrated in Figure 4.

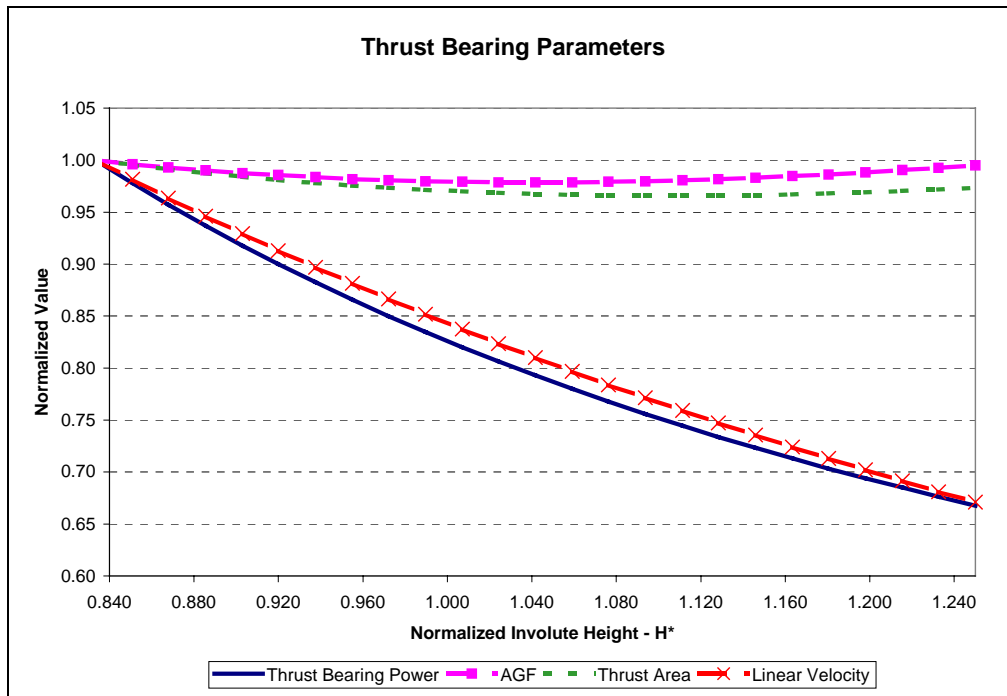


Figure 4. Thrust bearing parameters.

4.2 Radial Bearing Performance

The radial bearing power consumption is driven by the load and the constant film thickness requirement. For a design without radial compliance (i.e. fixed throw), the load on the orbiting scroll bearing (OSB) is largely made up of the vector sum of the orbiting scroll inertial load and the tangential gas load, with the radial gas load and other frictional loads having a less significant impact. While the decrease in orbiting scroll inertia presented in the previous section is certainly beneficial to the orbiting scroll bearing, it is offset by an increase in the tangential gas force (TGF). The major orbiting scroll bearing forces are shown in Figure 5.

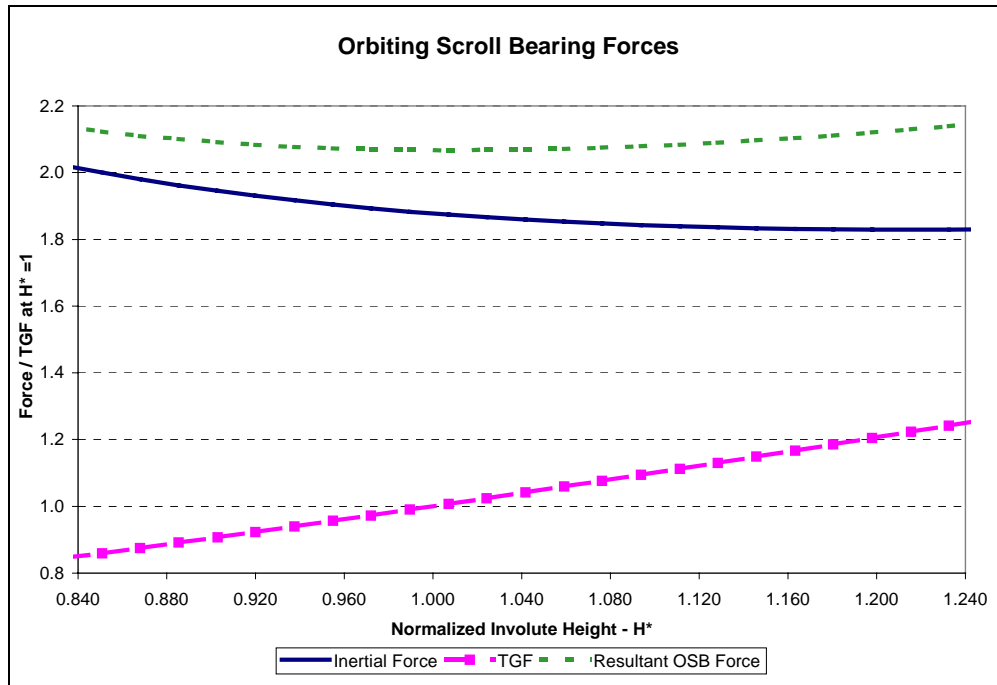


Figure 5. Orbiting scroll bearing forces.

Figure 5 shows that the load on the OSB is nearly constant over the range of heights and, therefore, not a significant contributor to the performance variation. Conversely, the load on the upper main bearing (UMB) and lower main bearing (LMB) increase significantly because the inertial load change has a minimal effect on their loads due to shaft counterweights. The loads on the main bearings are driven primarily by the TGF. To satisfy the constant film thickness constraint, sizes of the radial bearings are increasing with increasing load. The increase in bearing size causes an increase in power consumption. However, since the magnitude of the load on the LMB is low, a significant change in its load does not change its power consumption relative to the UMB or OSB significantly. The change in radial bearing power consumption for all three bearings is shown in Figure 6.

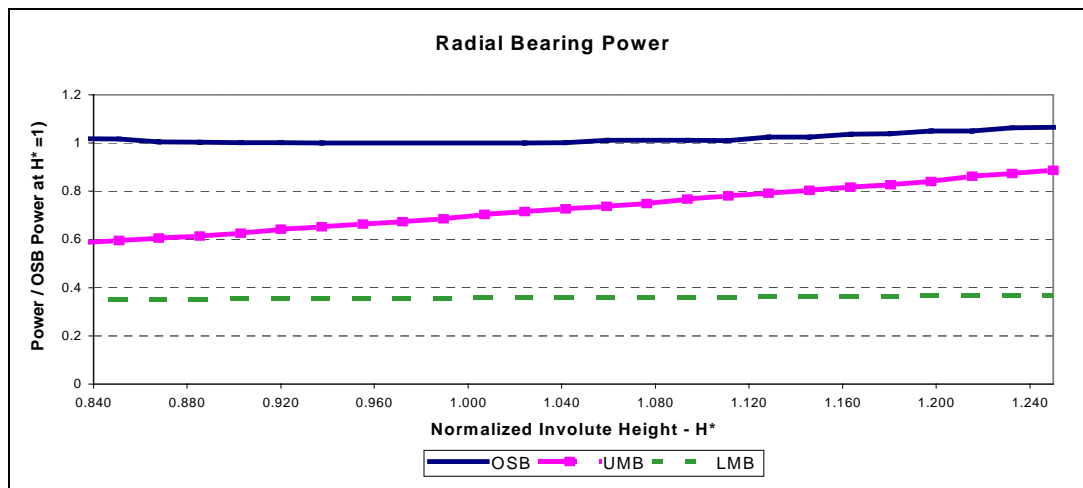


Figure 6. Radial bearing power consumption.

4.3 Leakage Considerations

The evaluation of leakage losses in the 1D model is based on a design which employs a tip seal and a fixed throw. As the involute height increases, the flank leakage term increases significantly and any change in overall leakage loss is dominated by this effect. The analysis is based on a constant flank gap assumption. The change in leakage loss is shown in Figure 7.

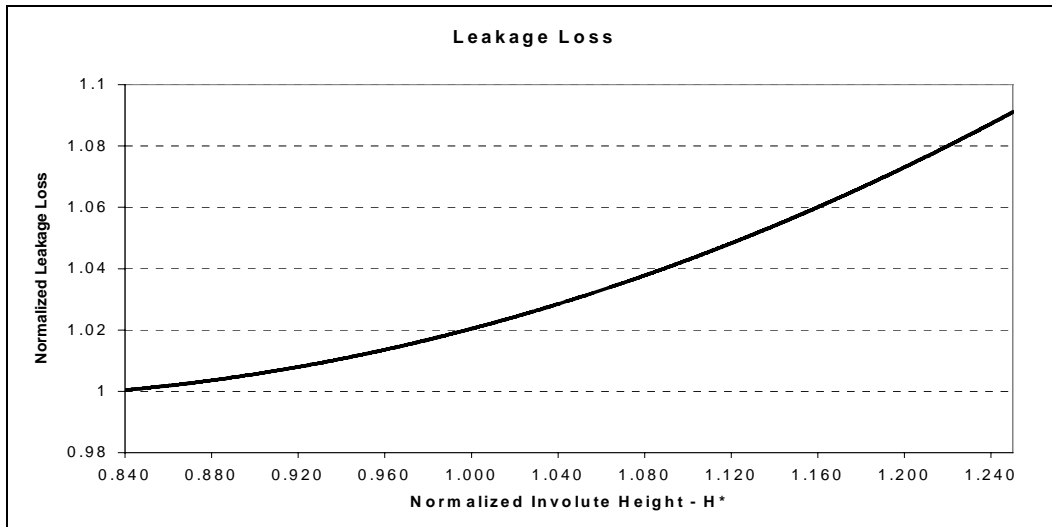


Figure 7. Leakage losses.

4.4 Performance Conclusions

The overall results of the 1D performance model were presented in Figure 3. The important characteristic of the performance curve is its relatively flat shape. Significant changes in involute height can take place without having a strong impact on performance. The results of the following section on machining considerations will aid in the selection of an involute geometry which provides reasonable performance without undue machining difficulty.

5. MACHINING CONSIDERATIONS

The machinability of the candidate geometries is evaluated based on estimated mill deflection. The mill deflection gives a relative measure of machining difficulty and potential for scrap generation. Previous work by Etemad and Nieter (1988) described a non-dimensional parameter for mill deflection defined as the involute height divided by the slot width. The method introduced here uses the involute height and the bending beam deflection equation to estimate the mill deflection, and the slot width geometry to determine the maximum allowable mill size. The maximum mill size selection is based on the slot width of the involute and an assumption of standard mill sizes. Since the slot size decreases as the involutes become taller, discontinuous increases in mill deflection will occur if the slot width decreases sufficiently to force a change to a smaller mill. The maximum allowable mill size for the considered range of involute heights is shown in Figure 8.

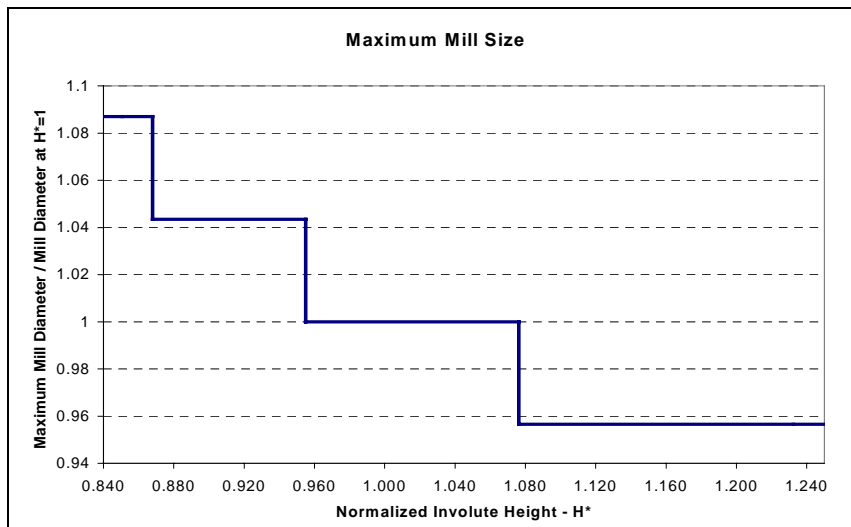


Figure 8. Maximum mill size.

The mill deflection model estimates the deflection at the mill tip by assuming a uniform distributed load on the mill where it contacts the flank wall. Since clearance is required between the chuck and flank tip, the mill is not loaded over its entire length. Therefore, Castigliano's theorem was used to develop equation (1) relating mill deflection and applied load.

$$\delta = \frac{q}{EI} \left(\frac{h_i^4}{24} + \frac{h_i h_m^3}{3} - \frac{h_m^2 h_i^2}{4} \right) \quad (1)$$

In equation (1) the variables represent the following: ' δ ', deflection at the mill tip; ' q ', uniform load applied along mill; ' E ', mill modulus; ' I ', mill moment of inertia; ' h_i ', height of involute; and ' h_m ', height of mill, which is the sum of the involute height and the clearance height. The values used for ' E ' and ' I ' are estimated based on material properties and cutter geometry, respectively. The value of the distributed applied load was determined by Manufacturing Engineering based on deflections observed in production processes. For each candidate geometry, equation (1) was used to estimate the mill deflection. The results are shown in Figure 9, which also includes the performance curve from Figure 3. With both curves included on the same plot, the compromise that can take place between performance and machinability in the geometry selection is well illustrated. A recommended geometry is also indicated in the figure.

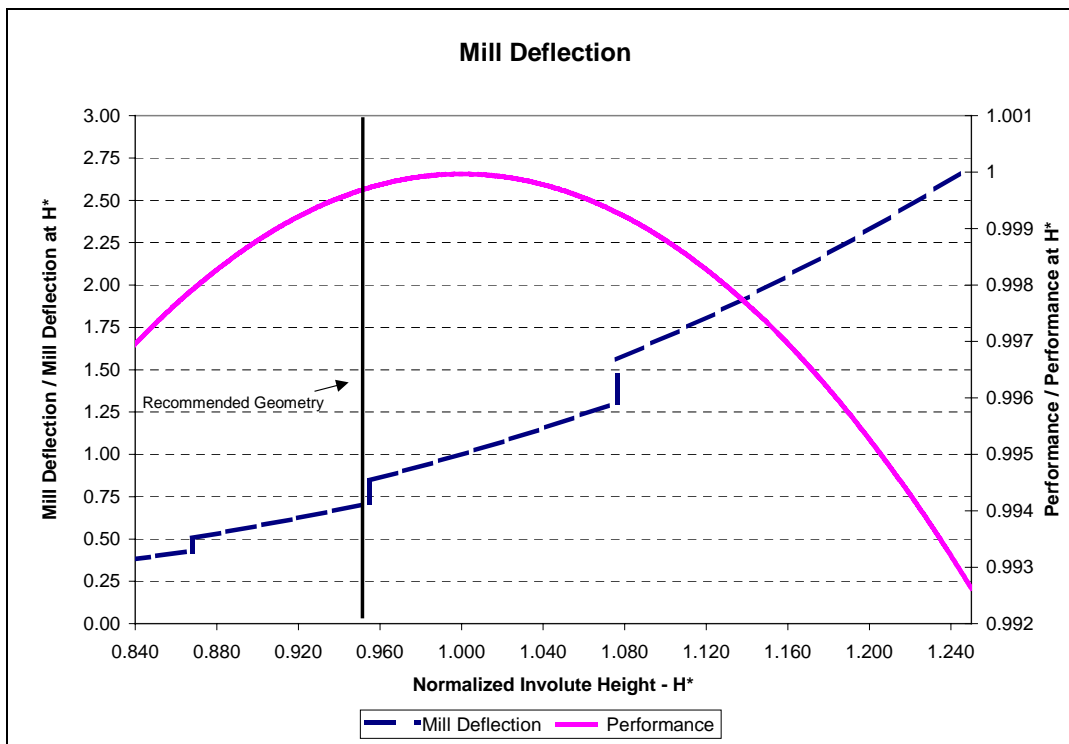


Figure 9. Mill deflection and performance results.

Based on the above analysis, the recommended geometry has at a normalized involute height of approximately 0.95 to take advantage of the largest mill size near the performance peak. The larger mill should allow incremental improvements in process control and scrap generation in the involute machining process.

6. CONCLUSIONS

This paper discussed an analytical method for the selection of an optimum involute height which considered both performance model results and machining considerations. From the group of candidate geometries used for illustration, a geometry was proposed which compromised little on performance but took advantage of standard tool size increments to decrease cutter deflections. Decreased cutter deflections should yield better process control and lower scrap generation.

The results also show the rate of performance change is low over the range of heights considered. Therefore, the designer has latitude in selecting a design based on machining considerations which compromises little on performance.

REFERENCES

- Etemad, S., Nieter, J., 1988, Computational Parametric Study of Scroll Compressor Efficiency, Design, and Manufacturing Issues, *1988 Int. Compressor Engineering Conference at Purdue*, vol. 1, p. 56-64
- Hemingway, E., 1965-66, The Measurement of Film Thickness in Thrust Bearings and the Deflected Shape of 'Parallel' Surface Thrust Pads, *Proceedings of the Institution of Mechanical Engineers*, vol. 180, part 1, no. 44: p. 1025-1054
- Ishii, N., Yamamoto, S., Muramatsu, S., Yamamura, M., Takahashi, M., 1992, Optimum Combination of Parameters for High Mechanical Efficiency of a Scroll Compressor, *1992 Int. Compressor Engineering Conference at Purdue*, vol. 1, p. 118a1-118a8
- Ishii, N., Yamamura, M., Muramatsu, S., Yamanda, S., Takahashi, M., 1994, A Study on High Mechanical Efficiency of a Scroll Compressor with Fixed Cylinder Diameter, *1994 Int. Compressor Engineering Conference at Purdue*, vol. 2, p. 677-682
- Ramondi, A., Boyd, J., 1958, A Solution for the Finite Journal Bearing and Its Application to Analysis and Design: III, *Transactions of American Society of Lubrication Engineers*, vol. 1, no. 1, in *Lubrication Science and Technology*, Pergamon, p.194-209
- Young, W., 1989, *Roark's Formulas for Stress & Strain*, 6th ed., McGraw-Hill, USA, 763 p.

ACKNOWLEDGEMENT

The author would like to thank Jack Sauls, Dan Crum, and Jerry Rood for the use of the models they created, which served as the foundation of this study.